Coherence Cloning Using Semiconductor Laser Optical Phase-Lock Loops

Naresh Satyan, Wei Liang, and Amnon Yariv, *Life Fellow, IEEE*

***Abstract*—We demonstrate the concept of coherence cloning where the coherence properties of a high-quality spectrally stabilized fiber laser are transferred to a commercially available high-power DFB semiconductor laser (SCL) using an optical phase-lock loop. The lineshapes and frequency noise spectra of the fiber laser and the free-running and phase-locked SCL are measured and compared. The bandwidth of coherence cloning is limited by physical factors such as the laser frequency modulation response and the loop propagation delay. The effect of this limited bandwidth on the laser field and on self-heterodyne interferometric measurements are analyzed.**

***Index Terms*—Optical interferometry, optical phase-lock loops (OPLLs), phase noise, semiconductor lasers (SCLs).**

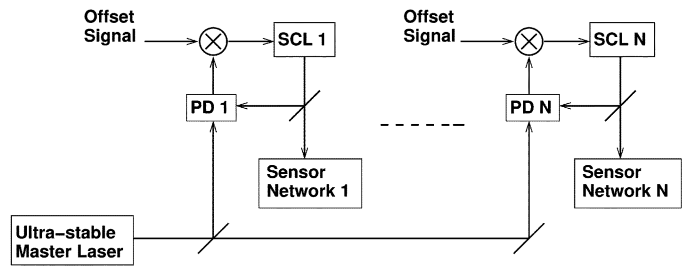

Fig. 1. Individual SCLs all lock to a common narrow-linewidth master laser, thus forming a coherent array. An offset RF signal is used in each loop for additional control of the optical phase (PD: photodetector).

I. Introduction

NARROW-LINEWIDTH fiber lasers and solid-state lasers have important applications in the area of fiber-optic sensing, interferometric sensing, light detection and ranging (LIDAR) measurement, etc. Semiconductor lasers (SCLs) are smaller, less expensive, operate at higher powers and are inherently more efficient compared to fiber lasers, dye lasers and solid-state lasers. However, they are much noisier due to their small volumes and the low reflectivity of the waveguide facet. The coherence properties of a high-quality master laser, such as a narrow-linewidth fiber laser, can be electronically cloned onto a number of noisy SCLs using optical phase-lock loops (OPLLs) [1], as shown in Fig. 1. This presents a significant advantage in applications that require a large number of spectrally stabilized laser sources. In this paper, we will describe the theoretical and experimental study of coherence cloning of a spectrally stabilized fiber laser to a high-power commercial semiconductor DFB laser using an OPLL. We will further analyze the impact of coherence cloning on the observed spectrum in a self-heterodyne Mach Zehnder interferometer (MZI). Such an experiment is very common, and is often used for laser lineshape and coherence characterization, as well as applications such as interferometric sensing and frequency-modulated continuous wave (FMCW) LIDAR.

Manuscript received August 14, 2008; revised October 23, 2008. Current version published May 28, 2009. This work was supported by the Defense Advanced Research Projects Agency's (DARPA) Microsystems Technology Office (MTO) and the Caltech Lee Center for Advanced Networking.

N. Satyan is with the Department of Electrical Engineering, California Institute of Technology, Pasadena, CA 91125 USA (e-mail: naresh@caltech.edu).

W. Liang is with OEwaves, Inc., Pasadena, CA 91106 USA (e-mail: wei.liang@oewaves.com).

A. Yariv is with the Department of Applied Physics and the Department of Electrical Engineering, California Institute of Technology, Pasadena, CA 91125 USA (e-mail: ayariv@caltech.edu).

Digital Object Identifier 10.1109/JQE.2009.2013120

II. Coherence Cloning

A. Theory

A schematic diagram of an OPPL is shown in Fig. 2(a). A slave local oscillator (LO) SCL is locked to a master laser at an offset frequency given by a reference RF oscillator. The propagation of phase noise in the loop is studied in the frequency domain using the theoretical model shown in Fig. 2(b). $F_f(f)$ and $F_{\rm FM}(f)$ are the transfer functions of the loop filter and the FM response of the SCL to input current, respectively, normalized to have unity gain at dc. $K_{\rm dc}$ is the total dc loop gain. $r(f)$ refers to the relative intensity noise (RIN) of the master laser. The RIN of the slave SCL is neglected in this analysis since the RIN of DFB SCLs is typically a few orders of magnitude smaller than the RIN peak that is usually present in fiber lasers at frequencies within the OPLL bandwidth. In our experiments, the DFB laser had a flat RIN spectrum of -135 dBc/Hz while the RIN peak of the master laser at 1 MHz was -115 dBc/Hz. When the loop is in lock, the frequency of the slave laser is given by $\omega_s = \omega_m - \omega_{\rm RF}$. ϕ_{e0} is the steady state phase error in the loop, and depends on the frequency difference $\Delta\omega$ between the master laser and the *free-running* slave SCL, offset by the RF oscillator frequency

$$\phi_{e0} = \sin^{-1}\frac{\Delta\omega}{K_{\rm dc}}. \quad (1)$$

The total small-signal loop gain $G_{op}(f)$ is given by

$$G_{op}(f) = \frac{K_{\rm dc}F_f(f)F_{\rm FM}(f)e^{-j2\pi f\tau_L}}{j2\pi f}. \quad (2)$$

Following a standard analysis [2] of the phase propagation in Fig. 2(b), we arrive at the following expression for the power

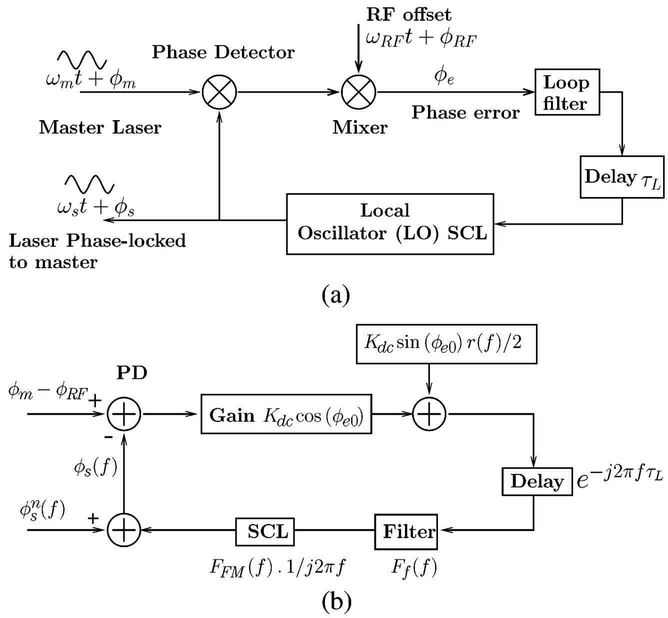

Fig. 2. (a) Schematic diagram of an OPLL. (b) Model for phase noise propagation in an OPLL.

spectral density (PSD) of the frequency noise of the locked slave laser

$$S_\nu^s(f) = S_\nu^m(f) \left| \frac{G_{op}(f) \cos \phi_{e0}}{1 + G_{op}(f) \cos \phi_{e0}} \right|^2 + S_\nu^{s,\mathrm{fr}}(f) \left| \frac{1}{1 + G_{op}(f) \cos \phi_{e0}} \right|^2 + f^2 \frac{S_{\mathrm{RIN}}^m(f)}{4} \left| \frac{G_{op}(f) \sin \phi_{e0}}{1 + G_{op}(f) \cos \phi_{e0}} \right|^2 \quad (3)$$

where $S_\nu^m(f)$, $S_\nu^{s,\mathrm{fr}}(f)$, and $S_{\mathrm{RIN}}^m(f)$ are the PSDs of the frequency noise of the master laser, the free-running slave laser, and the RIN of the master laser, respectively. The frequency noise ν is related to the phase noise ϕ by $\nu = (2\pi)^{-1} d\phi/dt$. The phase noise of the RF oscillator is very small compared to the laser phase noise, and is ignored. From (3), we find that for frequencies smaller than the loop bandwidth, where $|G_{op}(f)| \gg 1$, the phase noise of the SCL tracks the phase noise of the master laser. For frequencies greater than the loop bandwidth, $|G_{op}(f)| < 1$ and the SCL phase noise reverts to the free-running level.

B. Experiment

A commercial DFB laser (JDSU) is phase-locked to a narrow-linewidth fiber laser (NP Photonics) at an offset of 1.5 GHz using a heterodyne OPLL [3]. The OPLL is a Type I OPLL with a total loop propagation delay of about 6 ns. The FM response of the slave SCL shows a phase crossover [4] at 3 MHz, which limits the achievable loop bandwidth. A lag–lead filter is used in the loop to increase the dc gain, and hence the holding range of the OPLL. The filter has a transfer function of the form $(1 + j2\pi f \tau_2)/(1 + j2\pi f \tau_1)$ with a zero at $(2\pi\tau_2)^{-1} =$ 65 kHz, and a gain $\tau_1/\tau_2 \approx 50$. The rms residual phase noise (phase noise not corrected by the OPLL) is measured to be about 0.32 rad.

The phase noise of the master fiber laser and the free-running and phase-lock DFB slave laser are characterized using two measurements. The lineshapes of the lasers are measured using a delayed self-heterodyne interferometer with interferometer delay time much larger than the laser coherence time. The frequency noise spectra of the lasers are also directly measured using a fiber MZI as a frequency discriminator. The measured lineshapes of the fiber laser, and the free-running and locked DFB slave laser are plotted on a 50 MHz span in Fig. 3(a) and a 500-kHz span in Fig. 3(b). The lineshape of the master laser is normalized so that its peak is aligned with that of the phase-locked slave laser. The lineshape of the locked DFB laser is seen to be the same as the master fiber laser for frequencies less than 50 kHz. For frequencies above 50 kHz, the lineshape profile of the locked DFB laser does not completely track the fiber laser due to the limited bandwidth of the OPLL. The 20 dB linewidth of the DFB laser is reduced by more than two orders of magnitude from 4 MHz to 30 kHz. The finite-loop bandwidth limits the available phase margin at frequencies of ∼8 to 10 MHz, leading to a shoulder in the laser lineshape, as shown in Fig. 3(a). Moreover, the use of the lag–lead loop filter also reduces the phase margin at frequencies ∼100 kHz leading to noise peaks, as shown in Fig. 3(b).

The measured frequency noise spectra of the master fiber laser, and the free-running and locked slave DFB SCL are shown in Fig. 3(c). The frequency noise spectrum of the free-running slave SCL is about two orders of magnitude higher than that of the master laser, and shows additional noise peaks at the power line (60 Hz) harmonics and a spurious peak at 100 kHz due to a resonance in the laser driver circuit. The frequency noise spectrum of the locked DFB laser is reduced to a level identical to that of the fiber laser for frequencies less than 50 kHz, which is consistent with the observation of the lineshapes in Fig. 3(b). The measured frequency noise of the phase-locked DFB laser agrees well with the theoretical calculation (dashed curve) using (3).

We see, therefore, that the DFB laser emulates the linewidth and frequency noise spectrum of the master laser when phase-locked using a heterodyne OPLL. However, the coherence cloning is limited to frequencies within the bandwidth of the OPLL. The loop bandwidth is primarily limited by two factors, viz. the nonuniform FM response of a single-section SCL [4] and the loop delay [5], [6]. The limitation imposed by the loop delay can be relaxed by using miniature optics [7] and integrated electronics to reduce electronic rise times and optical and electronic propagation delays. The FM response of the laser poses a more serious concern, and previous efforts to demonstrate high-bandwidth SCL–OPLLs have only been successful using special multisection DFB lasers, which are expensive and not easily available. Efforts are in progress to overcome this limitation by exploring novel optical phase-locking architectures.

III. Coherence Cloning and Interferometer Noise

We will now consider the effect of a limited-bandwidth coherence cloning experiment on interferometer noise. In particular, we will consider the MZI shown in Fig. 4. The laser output is split into two arms of MZI with a differential delay T_d. One of

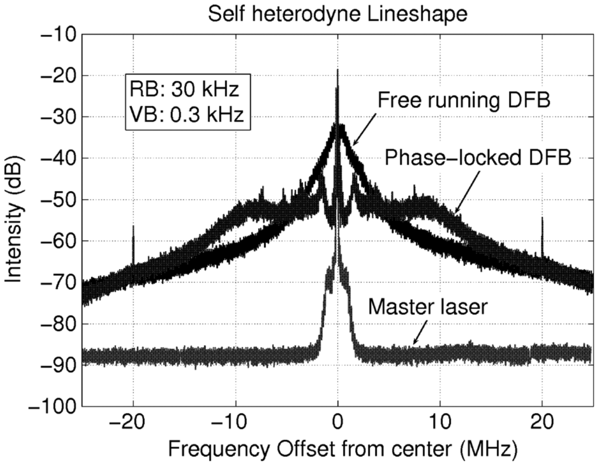

(a)

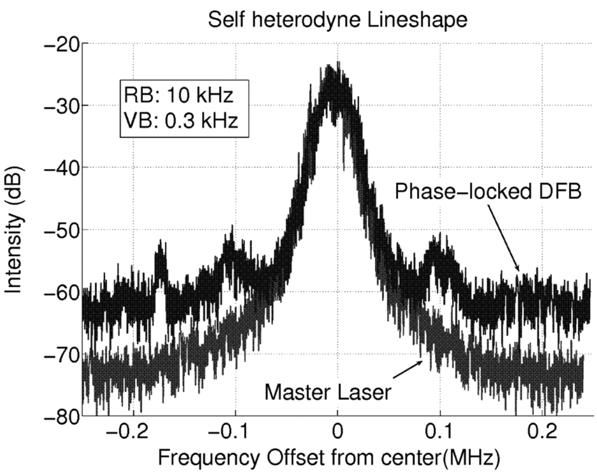

(b)

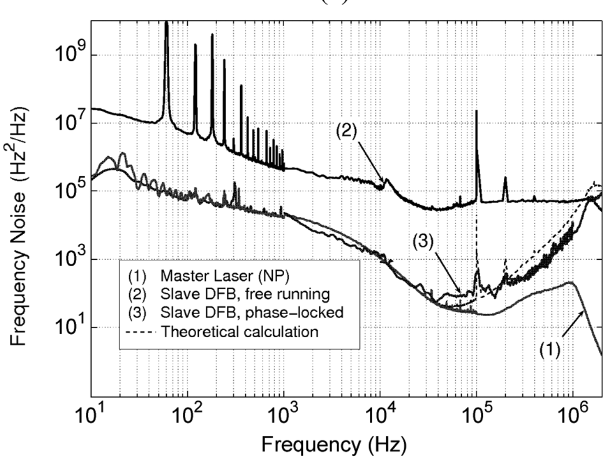

(c)

Fig. 3. (a) and (b) Measured lineshapes and (c) measured frequency noise spectra of the master fiber laser, and the free-running and phase-locked slave DFB SCL. The dashed curve in (c) is the theoretical calculation of the frequency noise spectrum of the phase-locked slave laser using (3).

the arms also has a frequency shifter, such as an electrooptic or acoustooptic modulator that shifts the frequency of the optical field by Ω. This delayed self-heterodyne configuration is very common in a number of applications such as laser lineshape characterisation, interferometric sensing, and FMCW LIDAR. The laser field is given by $e(t) = a(t)e^{j\omega_0 t+\phi(t)}$, where $a(t)$ is

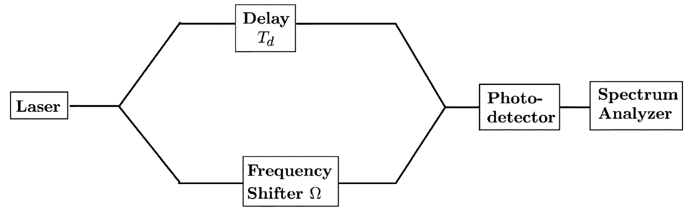

Fig. 4. Delayed self-heterodyne interferometer experiment.

the amplitude of the electric field, ω_0 the frequency of the laser, and $\phi(t)$ the laser phase noise. The output of the photodetector in Fig. 4 is given by

$$i(t) = \rho \left|e(t)e^{j\Omega t} + e(t-T_d)\right|^2. \tag{4}$$

The intensity noise of the laser is typically much smaller than the detected phase noise and is neglected in this analysis. Further, without loss of generality, we let $\rho = 1$ and $|a(t)| = 1$ so that the photodector current (around Ω) is given by

$$\begin{aligned} i(t) &= \Re\left(e^{j[(\omega_0+\Omega)t+\phi(t)]}e^{-j[\omega_0(t-T_d)+\phi(t-T_d)]}\right) \\ &= \Re\left(e^{j\omega_0 T_d}e^{j\Omega t}e^{j\Delta\phi(t,T_d)}\right) \end{aligned} \tag{5}$$

where $\Delta\phi(t,T_d) \doteq \phi(t) - \phi(t-T_d)$ is the accumulated phase in the time interval $(t-T_d, t)$. We wish to investigate the effect of coherence cloning on the spectrum of the electric field $e(t)$ and the photocurrent $i(t)$.

A. Coherence Cloning Model

Spontaneous emission in the lasing medium represents the dominant contribution to the phase noise $\phi(t)$ in a free-running SCL [8]. This gives rise to a frequency noise $\nu(t) = d/dt(\phi/2\pi)$ that has a PSD

$$S_\nu(f) = \frac{\Delta\nu}{2\pi} \tag{6}$$

which in turn leads to a Lorenzian spectrum for the laser electric field, with full-width at half-maximum (FWHM) $\Delta\nu$. In practice, there are also other noise sources that give rise to a $1/f$ frequency noise at lower frequencies, as can be seen from Fig. 3. It has been shown [9] that the optical field spectrum of a laser with $1/f$ frequency noise has a Gaussian lineshape as opposed to a Lorenzian lineshape. For simplicity of analysis, we will assume in this paper that the master and the free-running slave laser have flat frequency noise spectra corresponding to Lorenzian lineshapes with FWHMs $\Delta\nu_1$ and $\Delta\nu_2$, respectively, as shown in Fig. 5. Further, the OPLL is assumed to be an ideal OPLL with bandwidth f_L so that

$$G_{op}(f) = \begin{cases} \infty, & \text{if } f \le f_L \\ 0, & \text{if } f > f_L \end{cases}. \tag{7}$$

Using (3) and assuming that the effect of the master laser RIN is negligible (as is the case when $\phi_{e0} \ll 1$ even if $r(f)$ is non-negligible), we obtain

$$S_\nu^{\text{lock}}(f) = \begin{cases} \Delta\nu_1/2\pi, & \text{if } f \le f_L \\ \Delta\nu_2/2\pi, & \text{if } f > f_L \end{cases} \tag{8}$$

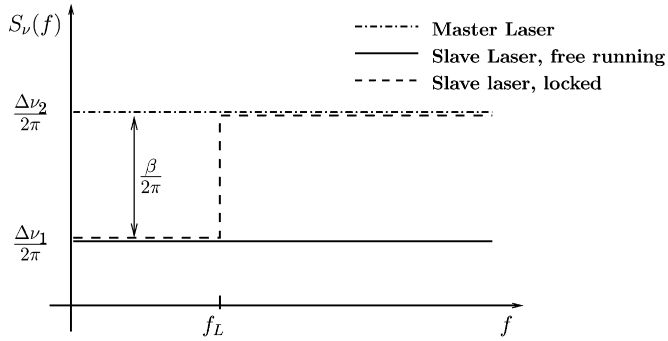

Fig. 5. Model of the PSD of the frequency noise of the master laser and the free-running and locked slave laser. The OPLL is assumed to be "ideal" with a loop bandwidth f_L.

as shown by the dashed curve in Fig. 5. We denote the reduction in linewidth by β

$$\beta = \Delta\nu_2 - \Delta\nu_1. \tag{9}$$

The accumulated phase noise $\Delta\phi(t, T_d)$ in (5) for a free-running laser is the result of a large number of independent spontaneous emission events that occur in the time interval $(t - T_d, t)$, and is therefore a zero mean Gaussian random process. Since the OPLL acts as a linear filter, the phase noise of an SCL phase-locked to a narrow-linewidth master laser in an OPLL also follows Gaussian statistics. The PSD of $\Delta\phi(t, T_d)$ is related to the PSD of the frequency noise by [10], [11]

$$S_{\Delta\phi(t,T_d)}(f) = 4\pi^2 T_d^2 S_\nu(f)\mathrm{sinc}^2(\pi f T_d) \tag{10}$$

with $\mathrm{sinc}(x) \doteq \sin x/x$, and its variance is given by

$$\sigma^2_{\Delta\phi}(T_d) = 4\pi T_d \int_{-\infty}^{\infty} S_\nu(f)\mathrm{sinc}^2(\pi f T_d)\pi T_d df. \tag{11}$$

Since $\Delta\phi(t, T_d)$ is a zero mean Gaussian process, its statistics [and therefore the statistics of the photocurrent in (5)] are completely determined by (11).

For a free-running laser with linewidth $\Delta\nu$ (6), we have from (11)

$$\sigma^2_{\Delta\phi}(T_d) = 2\pi\Delta\nu T_d. \tag{12}$$

Note that $\sigma^2_{\Delta\phi}(T_d)$ is an even function of T_d. For the phase-locked slave laser, we use (8) in (11) to obtain

$$\sigma^2_{\Delta\phi}(T_d) = 2\,\Delta\nu_2 T_d \int_{-\infty}^{\infty} \mathrm{sinc}^2(x)\,dx - 4\beta T_d \int_0^{\pi f_L T_d} \mathrm{sinc}^2(x)\,dx. \tag{13}$$

The second term in (13) quantifies the improvement in phase noise (or coherence) due to phase-locking, and is calculated by casting it in the form

$$\int_0^x \frac{\sin^2\alpha}{\alpha^2} d\alpha = -\frac{\sin^2 x}{x} + \mathrm{Si}(2x) \tag{14}$$

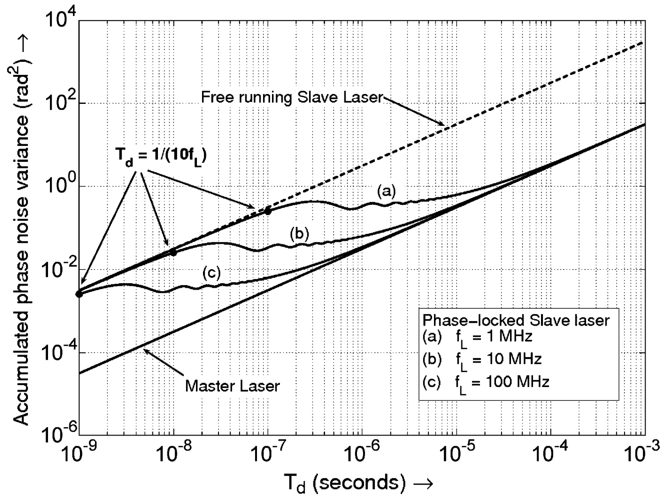

Fig. 6. Variation of the accumulated phase error variance $\sigma^2_{\Delta\phi}(T_d)$ versus interferometer delay time T_d for various values of the loop bandwidth f_L. The markers correspond to the delay time $T_d = 1/(10f_L)$. The linewidths of the master laser and the free-running slave laser are assumed to be 5 and 500 kHz, respectively.

where $\mathrm{Si}(x)$ is the well-known Sine integral $\int_0^x (\sin\alpha/\alpha)d\alpha$, whose value is numerically computed. The variation of $\sigma^2_{\Delta\phi}(T_d)$ versus T_d is calculated and plotted in Fig. 6. The values used in the calculation are $\Delta\nu_1 = 5$ kHz and $\Delta\nu_2 = 500$ kHz. The loop bandwidth f_L is varied between 1 and 100 MHz. It can be seen that $\sigma^2_{\Delta\phi}(T_d)$ follows the free-running slave laser for $T_d \lesssim (1/10f_L)$ and is approximately equal to that of the master laser for $T_d \gtrsim (100/f_L)$.

B. Spectrum of the Laser Field

We first calculate the shape of the electric field spectrum, i.e., the spectrum of $e(t) = \cos(\omega_0 t + \phi(t))$ for a free-running and phase-locked laser. To do this, we write down the autocorrelation of the electric field

$$\begin{aligned} R_e(\tau) &= \langle e(t)e(t-\tau)\rangle \\ &= \frac{1}{2}\langle\cos(\omega_0\tau)\cos(\Delta\phi(t,\tau))\rangle \\ &= \frac{\cos(\omega_0\tau)}{2}\exp\left(-\frac{\sigma^2_{\Delta\phi}(\tau)}{2}\right) \end{aligned} \tag{15}$$

where we have assumed that $\phi(t)$ is constant over one optical cycle and used the result $\langle\cos X\rangle = \exp(-\sigma_X^2/2)$ for a Gaussian random variable X. From the Wiener–Khintchine theorem, the spectrum of the electric field is given by the Fourier transform of (15). We define the spectrum at baseband by

$$S_{e,b}(f) = \mathcal{F}\left\{\exp\left(-\frac{\sigma^2_{\Delta\phi}(\tau)}{2}\right)\right\} \tag{16}$$

so that the two-sided PSD of the field $S_e(f)$ is given by

$$S_e(f) = \frac{1}{4}\left(S_{e,b}\left(f - \frac{\omega_0}{2\pi}\right) + S_{e,b}\left(f + \frac{\omega_0}{2\pi}\right)\right). \tag{17}$$

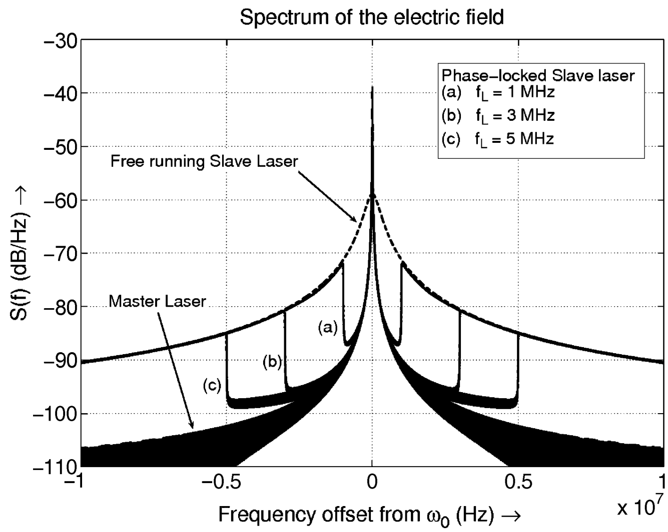

Fig. 7. PSD of the optical field for different values of the loop bandwidth f_L, calculated from (16). The master laser and the free-running slave laser have Lorenzian lineshapes with FWHM 5 and 500 kHz, respectively.

For a free-running laser, (12) and (16) yield the expected Lorenzian lineshape

$$S_{e,b}(f) = \frac{2}{\pi\Delta\nu}\frac{1}{1+(2f/\Delta\nu)^2}. \tag{18}$$

For the phase-locked laser, the field lineshape is calculated using (13) and (16), and is shown in Fig. 7 for different values of the loop bandwidth f_L. It can be seen that the lineshape of the phase-locked laser follows that of the free-running slave laser for frequencies $f \geq f_L$ and that of the master laser for frequencies $f \lesssim f_L$. This result is in good agreement with the experimentally measured lineshapes in Fig. 3. The earlier result can be intuitively understood by noting that for sufficiently large frequencies, the phase noise is much smaller than 1 rad. We can therefore make the approximation $\cos(\omega_0 t + \phi(t)) \approx \cos(\omega_0 t) + \phi(t)\sin(\omega_0 t)$, and the behavior of the field spectrum in this frequency range is therefore the same as that of the spectrum of the phase noise.

C. Spectrum of the Detected Photocurrent

We now calculate the spectrum of the photocurrent detected in the experimental setup of Fig. 4, i.e., the spectrum of the current $i(t)$ in (5)

$$i(t) = \cos\left(\omega_0 T_d + \Omega t + \Delta\phi(t, T_d)\right).$$

The autocorrelation of the photocurrent is derived similar to (15)

$$\begin{aligned}R_i(\tau) &= \langle i(t) i(t-\tau)\rangle \\ &= \langle \cos\left(\omega_0 T_d + \Omega t + \Delta\phi(t,T_d)\right) \\ &\qquad \times \cos\left(\omega_0 T_d + \Omega t - \Omega\tau + \Delta\phi(t-\tau, T_d)\right)\rangle \\ &= \frac{\cos\Omega\tau}{2}\exp\left(-\frac{\sigma_\theta^2(T_d,\tau)}{2}\right)\end{aligned} \tag{19}$$

where we define

$$\theta(t, T_d, \tau) \doteq \Delta\phi(t, T_d) - \Delta\phi(t-\tau, T_d). \tag{20}$$

In deriving (19), we have again made the assumption that Ω is much larger than the laser linewidth, and used the fact that θ follows Gaussian statistics. The variance of θ is given by

$$\begin{aligned}\sigma_\theta^2(T_d,\tau) &= \left\langle \theta^2(t, T_d, \tau)\right\rangle \\ &= \left\langle \Delta\phi^2(t,T_d) + \Delta\phi^2(t-\tau, T_d)\right. \\ &\qquad \left. -2\Delta\phi(t,T_d)\Delta\phi(t-\tau,T_d)\right\rangle \\ &= 2\sigma_{\Delta\phi}^2(T_d) - 2\left\langle\Delta\phi(t,T_d)\Delta\phi(t-\tau,T_d)\right\rangle.\end{aligned} \tag{21}$$

$$\begin{aligned}&\langle \Delta\phi(t,T_d)\Delta\phi(t-\tau,T_d)\rangle \\ &\quad = \langle\left(\phi(t)-\phi(t-T_d)\right)\left(\phi(t-\tau)-\phi(t-\tau-T_d)\right)\rangle \\ &\quad = \frac{1}{2}\left\langle \Delta\phi^2(t,\tau+T_d) + \Delta\phi^2(t-T_d,\tau-T_d)\right. \\ &\qquad\qquad \left. -\Delta\phi^2(t,\tau) - \Delta\phi^2(t-T_d,\tau)\right\rangle \\ &\quad = \frac{1}{2}\sigma_{\Delta\phi}^2(\tau+T_d) + \frac{1}{2}\sigma_{\Delta\phi}^2(\tau-T_d) - \sigma_{\Delta\phi}^2(\tau).\end{aligned} \tag{22}$$

Substituting back into (21), we have

$$\sigma_\theta^2(T_d,\tau) = 2\sigma_{\Delta\phi}^2(T_d) + 2\sigma_{\Delta\phi}^2(\tau) - \sigma_{\Delta\phi}^2(\tau+T_d) - \sigma_{\Delta\phi}^2(\tau-T_d). \tag{23}$$

We again define the baseband current spectrum

$$S_{i,b}(f) = \mathcal{F}\left\{\exp\left(-\frac{\sigma_\theta^2(T_d,\tau)}{2}\right)\right\} \tag{24}$$

so that the double-sided PSD of the photocurrent is given by

$$S_i(f) = \frac{1}{4}\left(S_{i,b}\left(f - \frac{\Omega}{2\pi}\right) + S_{i,b}\left(f + \frac{\Omega}{2\pi}\right)\right). \tag{25}$$

The case of a free-running laser has been studied previously by Richter *et al.* [12], where it was shown that for low values of T_d, the spectrum is characterized by a sharp delta function accompanied by a pedestal with oscillations whose period corresponds to the free spectral range of the interferometer. As the value of T_d increases, the strength of the delta function relative to the pedestal reduces, until a Lorenzian profile with FWHM $2\,\Delta\nu$ is obtained for $\Delta\nu T_d \gg 1/\pi$. For the phase-locked slave laser, we numerically calculate the spectra of the photocurrent using (24), (23), and (13). The results of the calculation are shown in Fig. 8. In general, the shape of the spectrum follows that of the master laser with the following important difference. For frequencies $\gtrsim$ the loop bandwidth f_L, the PSD of the phase-locked laser increases to the level of the free-running case. However, the features corresponding to the free spectral range of the interferometer are still present. The improvement in the coherence of the phase-locked SCL manifests itself in the presence of the delta function even at large delay times where the free-running laser results in a Lorenzian output.

In most practical sensing applications involving lasers, the delay time T_d is much smaller than the coherence time of the laser, in the regime shown in Fig. 8(a). In this case, the presence of a pedestal constitutes a deviation from the "ideal" case of a delta function, and represents unwanted noise in the interferometric sensing measurement. Comparing the spectra of the master laser and the phase-locked laser in Fig. 8(a), we see that the noise level is almost identical for small frequencies, but the

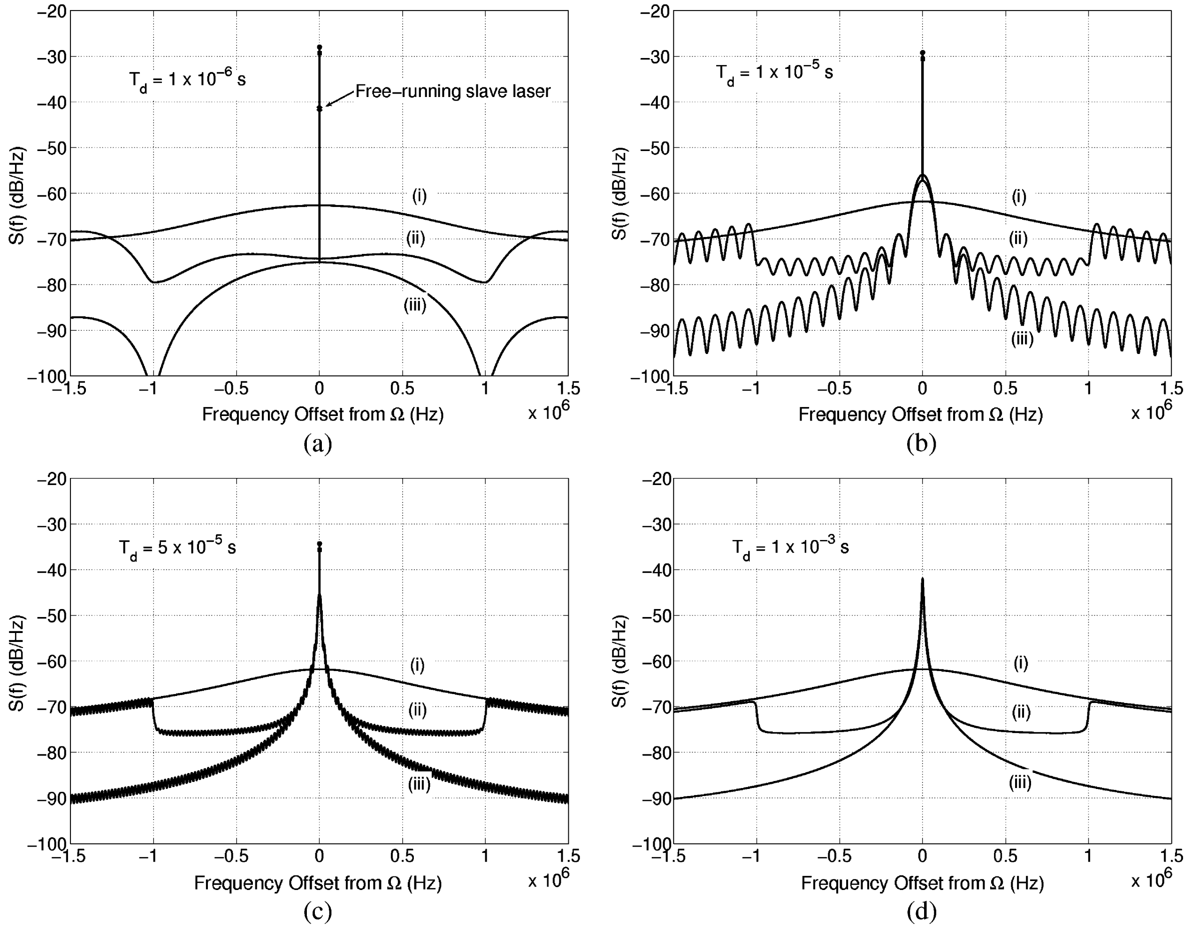

Fig. 8. PSD of the detected photocurrent in a self-heterodyne MZI using: i) the free-running slave laser; ii) the phase-locked slave laser; and iii) the master laser. The markers denote the height of the delta function. The spectra are calculated using (24), for different values of the interferometer delay T_d. (a) $T_d = 10^{-6}$ s. (b) $T_d = 10^{-5}$ s. (c) $T_d = 5 \times 10^{-5}$ s. (d) $T_d = 10^{-3}$ s. The master laser and free-running slave laser linewidths are assumed to be 5 and 500 kHz, respectively, and the loop bandwidth is assumed to be $f_L = 1$ MHz.

phase-locked laser has greater noise for frequencies $\gtrsim$ the OPLL bandwidth. However, this additional noise level is still many orders of magnitude below the delta function, and is outside the signal bandwidth so that it can be filtered out using a narrow bandwidth electrical filter.

IV. Conclusion

In conclusion, we have demonstrated the concept of "coherence cloning," i.e., the cloning of the spectral properties of a high-quality master laser to an inexpensive SCL, using an OPLL. The SCL is an attractive candidate for many interferometric applications because of its high responsivity to applied current, high power output, and compact size. The bandwidth over which the spectrum is cloned is limited by physical factors such as the FM response of the SCL and the OPLL propagation delay. Using a simple model for the coherence cloning, we have investigated the effect of this limited bandwidth on the spectrum of the laser electrical field, and on the result of interferometric experiments using the laser, which are common in many sensing applications. We have demonstrated that the spectrum of the field of the locked laser follows the master laser for frequencies lesser than the loop bandwidth, and follows the free-running spectrum for higher frequencies. We have further shown that a similar behavior is observed in interferometric experiments. Since the additional noise due to the limited loop bandwidth appears at high frequencies greater than the loop bandwidth, it can be electronically filtered off using a narrow bandwidth filter. Though these calculations were performed for a coherence cloning approach using OPLLs, the results are valid for any general linewidth-narrowing approach, since the bandwidth of linewidth reduction is always finite and limited by the propagation delay in the feedback scheme.

Acknowledgment

The authors would like to thank Dr. R. Lee, Orbits Lightwave, Inc., and Dr. A. Kewitsch and Dr. G. Rakuljic, Telaris, Inc., for many helpful discussions.

References

[1] A. Yariv, "Dynamic analysis of the semiconductor laser as a current-controlled oscillator in the optical phased-lock loop: Applications," *Opt. Lett.*, vol. 30, no. 17, pp. 2191–2193, 2005.

[2] F. M. Gardner, *Phaselock Techniques*, 3rd ed. New York: Wiley-Interscience, 2005.

[3] W. Liang, A. Yariv, A. Kewitsch, and G. Rakuljic, "Coherent combining of the output of two semiconductor lasers using optical phase-lock loops," *Opt. Lett.*, vol. 32, no. 4, pp. 370–372, 2007.

[4] P. Corrc, O. Girad, J. de Faria, and I. F. , "On the thermal contribution to the FM response of DFB lasers: Theory and experiment," *IEEE J. Quantum Electron.*, vol. 30, no. 11, pp. 2485–2490, Nov. 1994.
[5] R. T. Ramos and A. J. Seeds, "Delay, linewidth and bandwidth limitations in optical phase-locked loop design," *Electron. Lett.*, vol. 26, no. 6, pp. 389–391, Mar. 1990.
[6] M. Grant, W. Michie, and M. Fletcher, "The performance of optical phase-locked loops in the presence of nonnegligible loop propagation delay," *J. Lightw. Technol.*, vol. 5, no. 4, pp. 592–597, Apr. 1987.
[7] L. N. Langley, M. D. Elkin, C. Edge, M. J. Wale, U. Gliese, X. Huang, and A. J. Seeds, "Packaged semiconductor laser optical phase-locked loop (OPLL) for photonic generation, processing and transmission of microwave signals," *IEEE Trans. Microw. Theory Tech.*, vol. 47, no. 7, pp. 1257–1264, Jul. 1999.
[8] A. Yariv, *Quantum Electronics*, 3rd ed. New York: Wiley, 1988.
[9] M. J. O'Mahony and I. D. Henning, "Semiconductor laser linewidth broadening due to $1/f$ carrier noise," *Electron. Lett.*, vol. 19, no. 23, pp. 1000–1001, Oct. 1983.
[10] L. S. Cutler and C. L. Searle, "Some aspects of the theory and measurement of frequency fluctuations in frequency standards," *Proc. IEEE*, vol. 54, no. 2, pp. 136–154, Feb. 1966.
[11] K. Petermann, "Advances in optoelectronics (ADOP)," in *Laser Diode Modulation and Noise*. Dordrecht/Tokyo: Kluwer/KTK Scientific Publishers, 1991.
[12] L. Richter, H. Mandelberg, M. Kruger, and P. McGrath, "Linewidth determination from self-heterodyne measurements with subcoherence delay times," *IEEE J. Quantum Electron.*, vol. QE-22, no. 11, pp. 2070–2074, Nov. 1986.

Naresh Satyan received the B.Tech. degree in electrical engineering from the Indian Institute of Technology Madras, Chennai, India, in 2005, and the M.S. degree in electrical engineering from the California Institute of Technology, Pasadena, in 2007, where he is currently working toward the Ph.D. degree in electrical engineering.

His current research interests include optical phase-lock loops, semiconductor lasers, coherent optics, RF photonics, and optoelectronics.

Wei Liang received the B.S. degree from the Tsinghua University, Beijing, China, in 2001, and the M.S. and Ph.D degrees in applied physics from the California Institute of Technology, Pasadena, in 2003 and 2008, respectively.

He is currently with OEwaves, Inc., Pasadena, CA. His current research interests include phase- and frequency-locking of lasers, RF photonics, and coherent optics.

Amnon Yariv (S'56–M'59–F'70–LF'95) received the B.S., M.S., and Ph.D. degrees in electrical engineering from the University of California, Berkeley, in 1954, 1956, and 1958, respectively.

In 1959, he joined Bell Telephone Laboratories, Murray Hill, NJ. In 1964, he joined the California Institute of Technology, Pasadena, as an Associate Professor of electrical engineering, where he became a Professor in 1966. In 1980, he became the Thomas G. Myers Professor of electrical engineering and applied physics. In 1996, he became the Martin and Eileen Summerfield Professor of applied physics and Professor of electrical engineering. On the technical and scientific sides, he took part (with various coworkers) in the discovery of a number of early solid-state laser systems, the original formulation of the theory of nonlinear quantum optics, proposing and explaining mode-locked ultrashort-pulse lasers, GaAs optoelectronics; in proposing and demonstrating semiconductor-based integrated optics technology, pioneering the field of phase conjugate optics, and proposing and demonstrating the semiconductor DFB laser. He has authored or coauthored widely in the laser and optics fields and has written a number of basic texts in quantum electronics, optics, and quantum mechanics.

Dr. Yariv is a member of the American Academy of Arts and Sciences, the National Academy of Engineering, and the National Academy of Sciences.